Adiabatic light transfer in titanium diffused lithium niobate waveguides

H. P. Chung,[1] K. H. Huang,[1] S. L. Yang,[1] W. K. Chang,[1] C. W. Wu,[2] F. Setzpfandt,[3] T. Pertsch,[3] D. N. Neshev,[2] and Y. H. Chen[1,*]

[1]*Department of Optics and Photonics, National Central University, Jhongli 320, Taiwan*
[2]*Nonlinear Physics Centre, CUDOS, Research School of Physics and Engineering, Australian National University, Canberra, ACT 0200, Australia*
[3]*Institute of Applied Physics, Abbe Center of Photonics, Friedrich-Schiller-Universität Jena, 07743 Jena, Germany*
**yhchen@dop.ncu.edu.tw*

Abstract: We report on the realization of adiabatic light transfer in lithium niobate ($LiNbO_3$) waveguides. This peculiar adiabatic tunneling scheme was implemented in a three-waveguide coupling configuration with the intermediate waveguide being inclined with respect to the outer waveguides to facilitate the adiabatic passage process. We have investigated and determined the adiabatic conditions of the $LiNbO_3$ device in terms of the structure configuration of the waveguide system and found optimal structure parameters by both simulation and experimental approaches. Broadband adiabatic couplings of bandwidth ~456 and 185 nm and peak coupling efficiencies of >0.96 have been obtained with a 2-cm long device for TE- and TM-polarized fundamental modes, respectively. Longer (5 cm) devices were also studied and found to be useful in increasing the adiabaticity of the device, especially for the TM-polarized mode.

OCIS codes: (130.2790) Guided waves; (130.3730) Lithium niobate; (230.7380) Waveguides, channeled.

References and links

1. R. V. Schmidt and R. C. Alferness, "Directional coupler switches, modulators, and filters using alternating Δβ techniques," IEEE Trans. Circ. Syst. **26**(12), 1099–1108 (1979).
2. G. D. Valle, M. Ornigotti, T. T. Fernandez, P. Laporta, S. Longhi, A. Coppa, and V. Foglietti, "Adiabatic light transfer via dressed states in optical waveguide arrays," Appl. Phys. Lett. **92**(1), 011106 (2008).
3. K. Bergmann, H. Theuer, and B. W. Shore, "Coherent population transfer among quantum states of atoms and molecules," Rev. Mod. Phys. **70**(3), 1003–1025 (1998).
4. E. Paspalakis, "Adiabatic three-waveguide directional coupler," Opt. Commun. **258**(1), 30–34 (2006).
5. A. Salandrino, K. Makris, D. N. Christodoulides, Y. Lahini, Y. Silberberg, and R. Morandotti, "Analysis of a three-core adiabatic directional coupler," Opt. Commun. **282**(23), 4524–4526 (2009).
6. S. Y. Tseng and Y. W. Jhang, "Fast and robust beam coupling in a three waveguide directional coupler," IEEE Photonics Technol. Lett. **25**(24), 2478–2481 (2013).
7. S. Longhi, "Adiabatic passage of light in coupled optical waveguides," Phys. Rev. E Stat. Nonlin. Soft Matter Phys. **73**(2), 026607 (2006).
8. C. W. Wu, A. S. Solntsev, D. N. Neshev, and A. A. Sukhorukov, "Photon pair generation and pump filtering in nonlinear adiabatic waveguiding structures," Opt. Lett. **39**(4), 953–956 (2014).
9. Y. Lahini, F. Pozzi, M. Sorel, R. Morandotti, D. N. Christodoulides, and Y. Silberberg, "Effect of nonlinearity on adiabatic evolution of light," Phys. Rev. Lett. **101**(19), 193901 (2008).
10. S. Longhi, G. Della Valle, M. Ornigotti, and P. Laporta, "Coherent tunneling by adiabatic passage in an optical waveguide system," Phys. Rev. B **76**(20), 201101 (2007).
11. F. Dreisow, A. Szameit, M. Heinrich, R. Keil, S. Nolte, A. Tünnermann, and S. Longhi, "Adiabatic transfer of light via a continuum in optical waveguides," Opt. Lett. **34**(16), 2405–2407 (2009).
12. C. Ciret, V. Coda, A. A. Rangelov, D. N. Neshev, and G. Montemezzani, "Broadband adiabatic light transfer in optically induced waveguide arrays," Phys. Rev. A **87**(1), 013806 (2013).
13. C. Y. Huang, C. H. Lin, Y. H. Chen, and Y. C. Huang, "Electro-optic Ti:PPLN waveguide as efficient optical wavelength filter and polarization mode converter," Opt. Express **15**(5), 2548–2554 (2007).
14. R. C. Alferness, R. V. Schmidt, and E. H. Turner, "Characteristics of Ti-diffused lithium niobate optical directional couplers," Appl. Opt. **18**(23), 4012–4016 (1979).
15. W. K. Burns, P. H. Klein, E. J. West, and L. E. Plew, "Ti diffusion in Ti : $LiNbO_3$ planar and channel optical waveguides," J. Appl. Phys. **50**(10), 6175–6182 (1979).

#251855 Received 13 Oct 2015; revised 6 Nov 2015; accepted 6 Nov 2015; published 16 Nov 2015

16. S. Fouchet, A. Carenco, C. Daguet, R. Guglielmi, and L. Riviere, "Wavelength dispersion of Ti induced refractive index change in $LiNbO_3$ as a function of diffusion parameters," J. Lightwave Technol. **5**(5), 700–708 (1987).
17. J. Van Roey, J. van der Donk, and P. E. Lagasse, "Beam-propagation method: analysis and assessment," J. Opt. Soc. Am. **71**(7), 803–810 (1981).
18. H. Li, F. Zhou, X. Zhang, and W. Ji, "Picosecond Z-scan study of bound electronic Kerr effect in $LiNbO_3$ crystal associated with two-photon absorption," Appl. Phys. B **64**(6), 659–662 (1997).
19. R. C. Alferness and J. J. Veselka, "Simultaneous modulation and wavelength multiplexing with a tunable Ti:$LiNbO_3$ directional coupler filter," Electron. Lett. **21**(11), 466–467 (1985).

1. Introduction

Waveguide couplers are important photonic devices widely used in integrated optics for many applications. They are usually two parallel and closely lying waveguides in a common optical substrate performing directional coupling, useful in implementing optical processing functions including wavelength filtering, polarization mode selection, power division, switching, and modulation [1]. Waveguide couplers can also be configured in an arrayed waveguide structure consisting of more than two waveguides. Such waveguide arrays have been exploited to explore a variety of interesting wave coupling phenomena including an adiabatic light transfer effect [2]. Ideally, an adiabatic directional coupler (DC) performs a counterintuitive light transfer between the two outer waveguides (which are far apart with negligible possibility of direct coupling) of the system without the excitation of the intermediate waveguide(s). This peculiar adiabatic tunneling scheme is found to be an optical analogue of the stimulated Raman adiabatic passage (STIRAP) process [3] discovered in quantum physics. The process enables the coherent adiabatic transfer of population between two long-lived energy levels (eigenmodes) in an atomic/molecular system (corresponding to the modes of the two outer waveguides in an adiabatic DC system), achieved via an auxiliary intermediate state(s) (corresponding to the mode of the intermediate waveguide(s) in an adiabatic DC system), which is not populated during the adiabatic transfer.

Adiabatic DCs of several different waveguide array configurations [2, 4–7] have been studied theoretically and experimentally, mainly to optically realize the coherent tunneling adiabatic passage (CTAP) effect that is difficult to observe in quantum systems. In contrast to conventional waveguide DCs, adiabatic DCs are characterized by several unique features including the capability of almost complete power transfer in a (quasi-) monotonic (non-back conversion) fashion, a high tolerance to waveguide fabrication errors, and a low sensitivity to the wavelength permitting broadband operation [4, 6]. Previous studies on adiabatic DCs discussed several applications based on this unique CTAP effect. Most interesting, it has been proposed to spatially filter the pump from modally entangled photon pairs generated via the spontaneous parametric down-conversion (SPDC) process in a nonlinear-optical waveguide array system [8]. Using adiabatic coupling in such systems, generated photon-pair states without spurious pump photons can be achieved without the need to accurately control waveguide fabrication errors. The study in [8] introduces a scheme of applying the linear adiabatic light transfer mechanism to an integrated optical system with second-order (quadratic) nonlinearity, which is an advantageous technology integration to address new applications (e.g., quantum information in [8]) thanks to the versatility of nonlinear optical effects and related subjects.

So far, adiabatic DC devices have been built and demonstrated in only few materials such as glasses and semiconductors [2, 9–11]. Furthermore, the effect has been demonstrated in photoinduced waveguides in SBN [12] which features a quadratic nonlinearity but is not suited for integrated optics applications. Dielectric nonlinear materials such as $LiNbO_3$, $LiTaO_3$, and KTP have been widely used in nonlinear-optic applications, especially for nonlinear wavelength conversion, because of their wide transparent window from near-UV to mid-IR, relatively high nonlinearity (accessible by the quasi-phase-matching technique), stable chemical and mechanical properties, and high laser damage threshold (especially desired for waveguide devices usually supporting only few-micron sized modes to allow for higher power handling capacity). In this work, we report to the best of our knowledge the first experimental demonstration of a broadband adiabatic DC in the iconic dielectric quadric

#251855 Received 13 Oct 2015; revised 6 Nov 2015; accepted 6 Nov 2015; published 16 Nov 2015

nonlinear material, $LiNbO_3$. $LiNbO_3$ is a versatile substrate playing a significant role in integrated optics and waveguide optics; it is thus always desirable to demonstrate new photonic devices in $LiNbO_3$ to expand the applicability of the devices via accessing the powerful multiple optical-function integration capability of $LiNbO_3$. For example, one can integrate the adiabatic DCs developed in this work with an efficient SPDC via periodic poling in a common $LiNbO_3$ substrate to realize the novel system proposed in [8] on a chip. The potential of this platform can be further enhanced by integration of other demonstrated functional elements, e.g. a periodically poled lithium niobate (PPLN) electro-optic polarization mode converter [13] for manipulating the polarization states of the modal-entangled photon pairs on the chip.

2. Device design and structure parameters

We implemented the adiabatic DCs in a simple three-waveguide coupling configuration [5] on a *z*-cut $LiNbO_3$ substrate, as schematically shown in Fig. 1(a). The adiabatic coupling occurs between the two parallel outer waveguides (***a*** and ***c***) built along the crystallographic *x* axis, which are apart by a sufficiently long distance to suppress direct evanescent coupling. The energy exchange between waveguides ***a*** and ***c*** is mediated via waveguide ***b***, which is slightly oblique with respect to the outer waveguides. In the design, we have defined several parameters to configure the waveguide system shown in Fig. 1(a): L for the length of the coupler, S_{ac} for the distance between the inner-edges of the waveguides ***a*** and ***c***, $S_{ab}(x)$ and $S_{bc}(x)$ for the distances between the inner-edges of the waveguides ***a*** and ***b*** and the waveguides ***b*** and ***c***, respectively, $S_0 = S_{ab}(0) = S_{bc}(0)$ for the (inner-)edge-to-edge distance from the waveguide ***b*** to the waveguide ***a*** as well as to the waveguide ***c*** in the middle of the device (i.e., at $x = 0$), and $\Delta S = S_{ab}(-L/2)-S_{bc}(-L/2) = S_{bc}(L/2)-S_{ab}(L/2)$ (the structure is centrally symmetric with respect to point $(x,y) = (0,0)$ in this design). These structure parameters determine the coupling behavior of the waveguides and therefore the adiabaticity of light transfer in such a system. In general, two adiabatic coupling conditions are used as criteria in design for such a three-waveguide coupling scheme [4]; one is associated with the coupling strengths (coupling coefficients) among the waveguides, while the other is related to the slope of the inclined waveguide ***b***. The coupling coefficients between the waveguides ***a*** and ***b***, ***b*** and ***c***, and ***a*** and ***c*** can be expressed as [14]

$$\begin{aligned}
\kappa_{ab}(x) &= \frac{\pi}{2l_{c,ab}(x)} = \frac{\pi}{2l_{c0}e^{S_{ab}(x)/r}} = \kappa_0 e^{\alpha x},\\
\kappa_{bc}(x) &= \frac{\pi}{2l_{c,bc}(x)} = \frac{\pi}{2l_{c0}e^{S_{bc}(x)/r}} = \kappa_0 e^{-\alpha x},\\
\kappa_{ac} &= \frac{\pi}{2l_{c,ac}} = \frac{\pi}{2l_{c0}e^{S_{ac}/r}},
\end{aligned} \tag{1}$$

respectively. In Eq. (1), $l_{c,ab}$ is the coupling length for directional coupling [14] between waveguides ***a*** and ***b*** (the same definition applies to $l_{c,bc}$ and $l_{c,ac}$), l_{c0} and r are parameters depending on the waveguide characteristics (the three waveguides are identical in channel width and fabricated with the same fabrication process) and can be experimentally determined by characterizing separately fabricated conventional DCs (see below), $\kappa_0 = \kappa_{ab}(0) = \kappa_{bc}(0) = \pi / 2l_{c0}e^{S_0/r}$ (i.e., κ_{ab} is equal to κ_{bc} in the middle of the device), and $\alpha \equiv \Delta S/rL$ is related to the slope of the inclined waveguide ***b*** and therefore the adiabatic rate of the coupling process. The first (major) adiabatic condition thus applies to α for achieving a slow adiabatic light transfer in the system, given by

$$\gamma = \alpha / \kappa_0 = \Delta S / \kappa_0 rL << 1. \tag{2}$$

#251855 Received 13 Oct 2015; revised 6 Nov 2015; accepted 6 Nov 2015; published 16 Nov 2015

The second adiabatic condition is set to ensure a negligible direct coupling between waveguides ***a*** and ***c*** and a pure excitation of waveguide ***a*** at the input end of the coupler, given by

$$\kappa_{ac} \sim 0 \text{ and } \kappa_{ab}(-L/2) < \kappa_{bc}(-L/2) \text{ (or } \xi = \kappa_{ab}(-L/2)/\kappa_{bc}(-L/2) < 1). \quad (3)$$

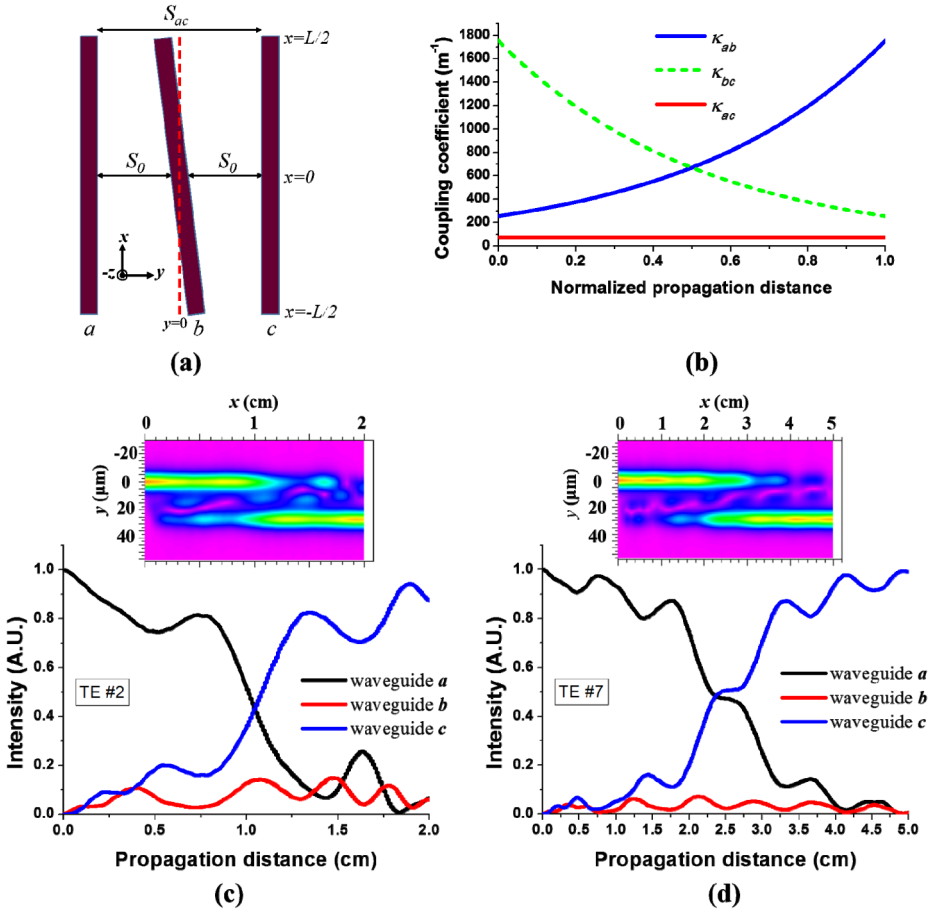

Fig. 1. (a) Schematic geometry of a three-waveguide adiabatic coupling system in a *z*-cut $LiNbO_3$. (b) Calculated coupling coefficients κ_{ab}, κ_{bc}, and κ_{ac} as a function of the wave propagation distance (along *x*) for the scheme with structure design parameters #2 for a TE-polarized 1550-nm fundamental mode. (c) and (d) are simulated evolutions of wave intensity in the schemes with structure design parameters #2 and #7 along the propagation distance for TE-polarized 1550-nm fundamental modes initially excited in waveguide ***a***, respectively (The insets show the corresponding evolutions of wave intensity in *x*-*y* plane in 2D color map).

In our work, we employed the titanium thermal diffusion (TTD) method [15] to fabricate the waveguide system shown in Fig. 1(a) in $LiNbO_3$. TTD has been one of the most popular technologies used to fabricate high-quality waveguides in $LiNbO_3$. Importantly, Ti-diffused $LiNbO_3$ waveguides support the guiding of both TE and TM modes, which allows for the investigation of the polarization dependence of the adiabatic coupling effect. To find proper design parameter values (see the scheme shown in Fig. 1(a)) for constructing adiabatic DCs in $LiNbO_3$, we first fabricated several conventional Ti:$LiNbO_3$ DCs with parallel waveguides of different interaction lengths (L_d) and waveguide separations (S_d) to experimentally derive the parameters l_{c0} and r. This is done by measuring the coupling efficiencies of the DCs as a function of L_d and S_d to deduce the coupling lengths (one S_d corresponds to one coupling length, at least two sets are required) and then the l_{c0} and r, which are independent of the

#251855 Received 13 Oct 2015; revised 6 Nov 2015; accepted 6 Nov 2015; published 16 Nov 2015

waveguide separation (see Eq. (1)) [14]. All the Ti:$LiNbO_3$ DCs were based on channel waveguides formed by high-temperature (1035°C) diffusion of Ti strips (95-nm thickness and 7-μm width) coated on the *-z* surface of a $LiNbO_3$ crystal. The waveguides support single-mode guiding of waves in the spectral range 1400-1700 nm for both TE and TM polarizations. More detailed information regarding the fabrication process and dispersion characterization of Ti-diffused $LiNbO_3$ waveguides can be found in [13] and [16]. We determined l_{c0} and r to be, for example at 1550-nm wavelength, 0.584 (0.665) mm and 4.677 (4.423) μm for the TE (TM)-polarized fundamental mode, respectively.

Table 1. Calculated adiabatic condition parameters for several different structure parameters for both polarizations modes at 1550 nm

Design number	Structure parameters			Adiabatic condition parameters					
				TE mode			TM mode		
#	L (mm)	S_{ac} (μm)	ΔS (μm)	γ	ξ	$\vartheta = \gamma\xi$	γ	ξ	$\vartheta = \gamma\xi$
1	20	20	8	0.1276	0.1808	0.0231	0.1664	0.1639	0.0273
2	20	20	9	0.1436	0.1460	0.0210	0.1872	0.1307	0.0245
3	20	22	8	0.1580	0.1808	0.0286	0.2086	0.1639	0.0342
4	20	22	9	0.1778	0.1460	0.0260	0.2347	0.1307	0.0307
5	20	22	10	0.1975	0.1179	0.0233	0.2608	0.1042	0.0272
6	20	22	11	0.2173	0.0952	0.0207	0.2869	0.0832	0.0239
7	50	22	11	0.0869	0.0952	0.0083	0.1147	0.0832	0.0095
8	50	18	6	0.0309	0.2773	0.0086	0.0398	0.2575	0.0103

With these derived waveguide-characteristics dependent parameters, we are able to find possible structure parameters for the adiabatic DC system, mainly $S_{ab}(x)$, $S_{bc}(x)$, and S_{ac} (or simply ΔS and S_{ac}), satisfying the adiabatic conditions under a fixed device length of L = 20 mm and a fixed waveguide channel width of W = 7 μm. Though a longer device length is preferable for a better adiabaticity according to the adiabatic condition given in Eq. (2), we use L = 20 mm due to the limit of our furnace capacity for processing the TTD. Nevertheless, this length already allows us to observe a broadband (in comparison to a conventional DC) adiabatic light transfer process for the first time in $LiNbO_3$ (see below). Table 1 lists the calculation results of the adiabatic condition parameters (γ and ξ in Eqs. (2) and (3), respectively) using Eq. (1) for several different S_{ac} and ΔS values for both polarizations modes at 1550-nm wavelength. The results show that (*i*) ξ is independent of S_{ac}; (*ii*) the increase of S_{ac} will increase the adiabaticity due to the decrease of κ_{ac} (the second adiabatic condition given in Eq. (3)) but will be detrimental to fulfillment of the first adiabatic condition given in Eq. (2) due to the decrease of κ_0; (*iii*) the increase and decrease of ΔS are detrimental to fulfillment of the first and second adiabatic conditions, respectively, according to Eqs. (2) and (3). Accordingly, we found that optimal values of S_{ac} and ΔS (leading to a minimal overall adiabatic condition parameter $\vartheta \equiv \gamma\xi$) are either around 20 and 9 μm (#2 in Tab. 1; ϑ = 0.0210 for TE mode and ϑ = 0.0245 for TM mode) or around 22 and 11 μm, respectively (#6 in Tab. 1; ϑ = 0.0207 for TE mode and ϑ = 0.0239 for TM mode). Figure 1(b) shows the calculated coupling coefficients κ_{ab}, κ_{bc}, and κ_{ac} according to Eq. (1) as a function of the TE wave propagation distance (along x) for the scheme with structure design parameters #2 (with ϑ = 0.0210) listed in Tab. 1. The corresponding evolution of the wave intensity in such a waveguide scheme for TE-polarized 1550-nm fundamental mode initially excited in waveguide ***a*** is simulated using the "Beam Propagation" method (BPM) [17] and plotted in Fig. 1(c). The simulated intensity evolution for a longer (5-cm long) scheme with structure design parameters #7 is also plotted in Fig. 1(d) for comparison. The simulated intensity evolution dynamics agrees with the typical adiabatic light transfer phenomenon observed in three-waveguide adiabatic DCs [5] and show, that the longer device does exhibit

#251855 Received 13 Oct 2015; revised 6 Nov 2015; accepted 6 Nov 2015; published 16 Nov 2015

a clearer signature of an adiabatic coupler (with much less excitation to the middle waveguide). The device length effect will be further investigated in the next section.

3. Device fabrication and output performance characterization

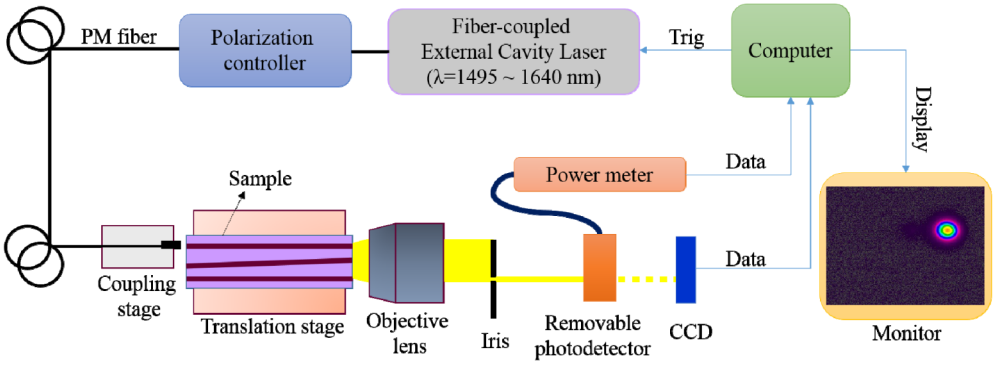

Fig. 2. Schematic arrangement of the measurement setup.

We fabricated six three-waveguide adiabatic DCs, adopting the structure designs from #1 to #6 listed in Tab. 1, respectively, in the same $LiNbO_3$ chip of 20-mm in length, 5-mm in width, and 0.5-mm in thickness. The end faces of the $LiNbO_3$ chip were optically polished, no optical coating was applied. The characteristics of the fabricated $LiNbO_3$ adiabatic DCs were then investigated by using an external cavity laser (linearly polarized, tunable between 1495 and 1640 nm) followed by a polarization controller (PC). The output of the PC was butt coupled into a waveguide of the $LiNbO_3$ adiabatic DCs via a polarization-maintaining fiber. The crystal was mounted on a multi-axis precision translation stage. The output powers and mode profiles from the three-waveguide system were measured using a photodetector (removable) and an optical mode profiler system (with an Infrared CCD camera), respectively. An objective lens and an iris system were used to facilitate the selection of one or all of the output modes for investigation. Figure 2 shows the schematic of the measurement setup. During our measurements we have kept the input power <~1 mW to avoid nonlinear effects [9] (we estimated the Kerr effect induced refractive index change is on the order of 10^{-11} at this power level [18], which is much smaller than that caused by Ti-diffusion process (0.005~0.02) [14]). First, we aligned the laser to excite only the waveguide ***a*** of each adiabatic DC. Figure 3 shows the measured and simulated (via BPM method) cross-coupling efficiencies (***a*** to ***c***) as a function of the excitation wavelength (1495-1640 nm) for some of the adiabatic DCs built in the sample. The cross-coupling efficiency is an index related to the adiabaticity of the system and defined as $\eta = \frac{P_c}{P_a + P_b + P_c}$, where P_a, P_b, and P_c are the measured output powers from the waveguides ***a***, ***b***, and ***c***, respectively. The results for the structure design #6 for TM mode are not shown because its peak coupling efficiency lies outside of the wavelength tuning range of our laser, though the structure is identified to have a minimal ϑ as discussed above. The experimental results are in good agreement with our simulations. Our results show that the coupling efficiencies of adiabatic DCs of different designs are less dependent on the structure parameters (S_{ac} and ΔS) and excitation wavelength for TE mode (Fig. 3(a)) than for TM mode (Fig. 3(b)). This is consistent with the calculated overall adiabatic condition parameters ϑ listed in Tab. 1 indicating that lower ϑ values are always obtained with the TE mode compared to the TM mode under the same structure parameters. Lower ϑ implies a better adiabaticity of the design and therefore a broader working bandwidth, as was experimentally confirmed by the results depicted in Fig. 3. The highest average coupling efficiencies (over the measured wavelength range) were obtained from the adiabatic DC with the structure design #2 (L = 20 mm, W = 7 μm, S_{ac} = 20 μm, and

#251855 Received 13 Oct 2015; revised 6 Nov 2015; accepted 6 Nov 2015; published 16 Nov 2015

ΔS = 9 μm) for both polarizations, which are η~0.88 and 0.84 for TE- and TM-mode excitations, respectively. This structure scheme has minimal ϑ values (for 2-cm long devices) and peak coupling efficiencies lying near 1550 nm for both polarizations. Figure 4 shows the captured output mode intensity profiles from the adiabatic DC with the structure design #2 at several different excitation wavelengths. It clearly shows that the majority of the energy has been transferred from input waveguide ***a*** to waveguide ***c*** so that only the output mode from waveguide ***c*** was sensed by the beam profiler over the scanning wavelength range (stopped at 1600 nm due to the detection limit of the beam profiler) using the TE-mode excitation (Fig. 4(a)). A similar transfer effect can be observed for TM-mode excitation (Fig. 4(b)), however, with narrower spectral range (~1560-1600 nm). The results shown in Fig. 4 confirm the observations made on Fig. 3, that the adiabaticity of the device is polarization dependent as a result of the discrepancy in waveguide dispersion between the two polarization modes [16].

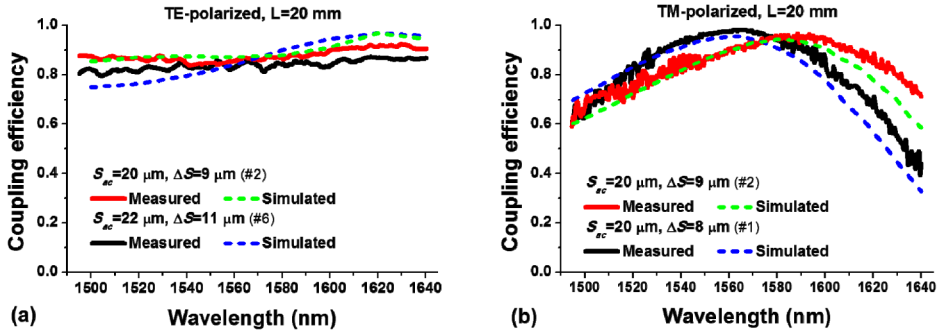

Fig. 3. Measured and simulated coupling efficiencies as a function of excitation wavelength for (a) structure design #2 and #6 with TE mode excitation and for (b) structure design #1 and #2 with TM mode excitation.

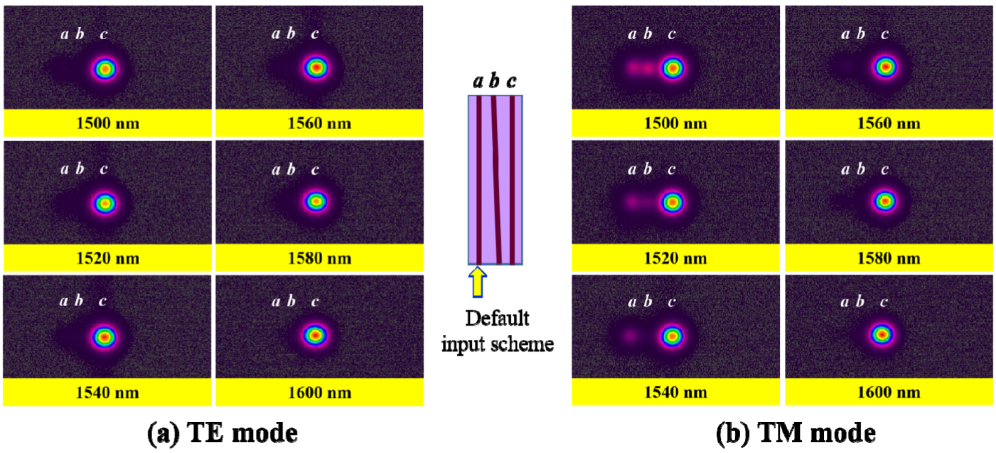

Fig. 4. Captured output mode intensity profiles from the adiabatic DC with the structure design #2 at several different excitation wavelengths. (a) Results for the TE-mode excitation. (b) Results for TM-mode excitation.

It is also interesting to explore the coupling process of the device when initially the light is launched into waveguide ***c*** (inverted injection scheme) instead. Figure 5(a) shows the measured output powers (normalized to total output power $P_a + P_b + P_c$) from the waveguides ***a*** and ***b*** of the same adiabatic DC (i.e., with the structure design #2) as a function of the wavelength in such an inverted light injection scheme (only results with TE-mode excitation are shown for illustration). Some of the corresponding output mode profiles of this measurement are also shown in Fig. 5(b). These measurements show that the typical

#251855 Received 13 Oct 2015; revised 6 Nov 2015; accepted 6 Nov 2015; published 16 Nov 2015

tunneling of light between the outer waveguides ***c*** and ***a*** does not occur over the scanned wavelength range. Instead, significant power also exits the sample from waveguide ***b***. The power in waveguide ***c*** is eventually transferred to both waveguides ***a*** and ***b*** [5].

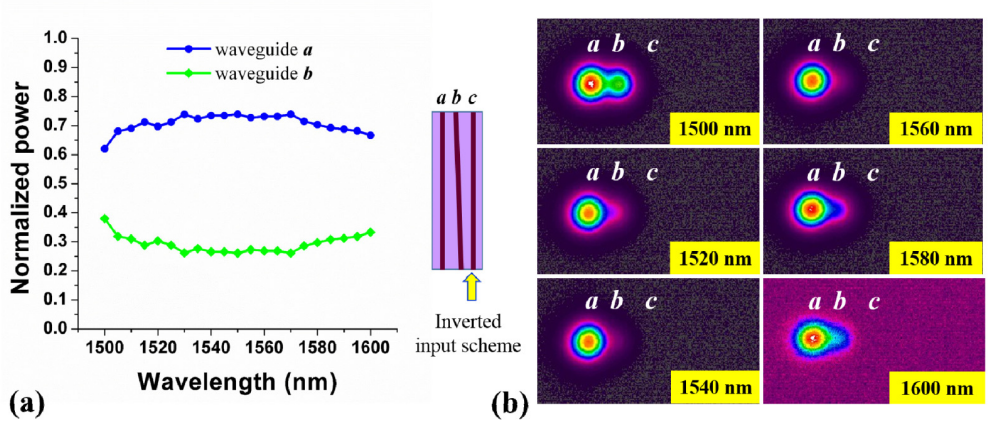

Fig. 5. (a) Measured normalized output powers from the waveguides ***a*** and ***b*** of the adiabatic DC with the structure design #2 in an inverted injection scheme as a function of the wavelength (TE-mode excitation). (b) Corresponding output mode intensity profiles at several different excitation wavelengths.

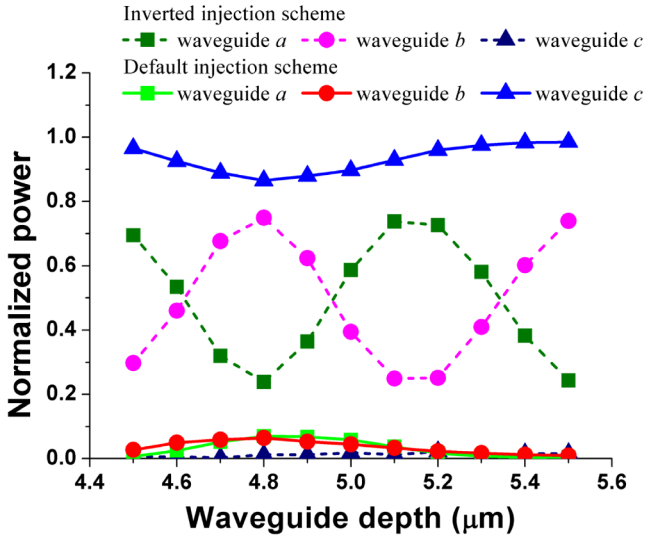

Fig. 6. Calculated normalized output powers from the three output ports of the $LiNbO_3$ adiabatic DC with the structure design #2 versus the waveguide depth for the default and inverted injection schemes with a TE-polarized 1550 nm wave.

To further demonstrate the practical usefulness of adiabatic coupling, we investigate the dependence of the coupler output on the waveguide fabrication parameters. Figure 6 shows the calculated normalized output powers (normalized to total output power) from the three output ports of the $LiNbO_3$ adiabatic DC with the structure design #2 versus the waveguide depth for the default and inverted injection schemes (i.e., injection into waveguides ***a*** and ***c***, respectively) with a TE-polarized 1550 nm wave. The behavior of the power exchange between waveguides ***a*** and ***b*** with respect to the waveguide depth found in the inverted injection scheme can be understood from the prediction made in [5] showing the power (transferred from waveguides ***c***) also exchanges between waveguides ***a*** and ***b*** as the waves

#251855 Received 13 Oct 2015; revised 6 Nov 2015; accepted 6 Nov 2015; published 16 Nov 2015

propagate towards the outputs of a similar three-waveguide system in the inverted injection scheme (i.e., in a fashion similar to the directional coupling, which is interaction length dependent). In our case, the change of the waveguide depth is equivalent to the change of the effective interaction length of a DC as the effective refractive index of the waveguide is changed. In addition, since waveguide depth is a sensitive function of the waveguide fabrication process, the results shown in Fig. 6 manifest that an adiabatic DC in the correct injection scheme features lower sensitivity to the fabrication error than in the inverted coupling scheme, another advantage besides having the least power coupled to the intermediate waveguide.

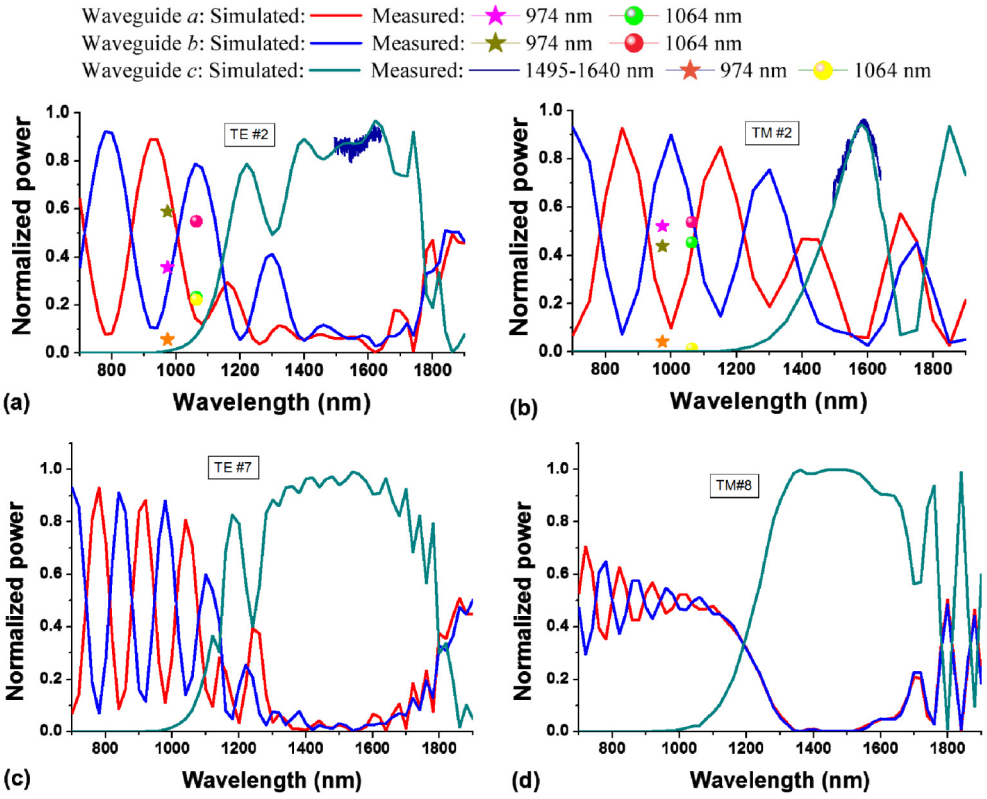

Fig. 7. Calculated normalized output powers from the three output ports of the $LiNbO_3$ adiabatic DCs with the structure design #2, #7, and #8 as a function of wavelength over 700-1900 nm. Measured data at 974, 1064, and 1495-1640 nm for design #2 are also plotted for comparison. (a) Design #2 (2 cm long device) with TE mode excitation. (b) Design #2 (2 cm long device) with TM mode excitation. (c) Design #7 (5 cm long device) with TE mode excitation. (d) Design #8 (5 cm long device) with TM mode excitation.

The successful modeling of the $LiNbO_3$ adiabatic DCs above allows us to further investigate the effect of the device length on the performance of the device. Figure 7 shows the calculated normalized output powers from the three output ports of the $LiNbO_3$ adiabatic DCs with the structure design #2, #7, and #8 (see Tab. 1) as a function of wavelength over a much wider spectral range than is accessible experimentally - 700-1900 nm. The measured data shown in Fig. 3 and additional measurement results obtained with 974 nm and 1064 nm cw lasers are also plotted for comparison. The data points at 974 and 1064 nm exhibit some shift from the calculation mainly because of a less accurate prediction of the waveguide dispersion (for both TE and TM modes) in this relatively shorter wavelength range. Nevertheless, the measured data agree very well with the calculated results in the tendency of the coupling behavior of such devices with respect to the wavelength. The results shown in

#251855 Received 13 Oct 2015; revised 6 Nov 2015; accepted 6 Nov 2015; published 16 Nov 2015

Fig. 7 reveal that the increase of the waveguide length is an effective approach to increase the adiabaticity of the device, as also suggested by Eq. (2). Longer devices lead to the broadening of the coupling bandwidth from ~456 and 185 nm at −3 dB for the 2-cm device to ~537 and 547 nm for the 5 cm device for TE and TM polarization modes, respectively, as well as to enhancement of the coupling efficiency from >0.96 maximally for the 2-cm device to >0.99 maximally for the 5 cm device for TE and TM polarization modes, respectively. The length effect (related to the adiabaticity) is especially remarkable for TM-mode excitation in Ti-diffused $LiNbO_3$ waveguides due to the dispersion characteristic of the polarization in the material. The obtained coupling bandwidths of the adiabatic DCs are overwhelmingly broader than in conventional DCs [19].

4. Conclusion

We have designed and fabricated adiabatic DCs in Ti-diffused $LiNbO_3$ waveguides and successfully demonstrated the adiabatic light tunneling process in such devices consisting of three waveguides, where the adiabatic coupling occurs between the two (far apart) outer waveguides via an intermediate waveguide slightly oblique with respect to the outer waveguides. The optimal structure parameters for 2-cm long $LiNbO_3$ adiabatic DCs were found to be S_{ac} = 20 μm and ΔS = 9 μm for both TE- and TM-polarized fundamental modes. The developed $LiNbO_3$ adiabatic DCs are characterized by three important features in contrast to conventional DCs: absence of back conversion of coupled energy, high tolerance to waveguide fabrication errors, and ultra-broad coupling bandwidth. The study also shows that the device adiabaticity can be effectively enhanced by increasing the device length, e.g., the coupling bandwidth is broadened from ~185 nm for a 2-cm device to ~547 nm for a 5 cm device, while the peak coupling efficiency is enhanced from >0.96 for the 2-cm device to >0.99 for the 5 cm device for the TM-polarized mode.

Acknowledgments

This work was supported by the Ministry of Science and Technology (MOST) of Taiwan under Contract Nos. 102-2221-E-008-099-MY2 and 104-2221-E-008-094, by the Australian Research Council through Discovery and Centre of Excellence programs, and by the German Academic Exchange Service (NSC-DAAD: 102-291-I-100-523).

#251855 Received 13 Oct 2015; revised 6 Nov 2015; accepted 6 Nov 2015; published 16 Nov 2015